


 Cite this: *RSC Adv.*, 2024, 14, 14456

# Fabrication of $-\text{SO}_3\text{H}$ -functionalized polyphosphazene-reinforced proton conductive matrix-mixed membranes†

 Jamal Afzal,  Jiashun Zhang and Haijiang Wang \*

Proton exchange membranes (PEMs) have emerged as very promising membranes for automotive applications because of their notable proton conductivity at low temperatures. These membranes find extensive utilization in fuel cells. Several polymeric materials have been used, but their application is constrained by their expense and intricate synthetic processes. Affordable and efficient synthetic methods for polymeric materials are necessary for the widespread commercial use of PEM technology. The polymeric combination of hexachlorocyclotriphosphazene (HCCP) and 4,4-diamino-2,2-biphenyldisulfonic acid facilitated the synthesis of PP-(PhSO<sub>3</sub>H)<sub>2</sub>, a polyphosphazene with built-in  $-\text{SO}_3\text{H}$  moieties. Characterization revealed that it was a porous organic polymer with high stability. PP-(PhSO<sub>3</sub>H)<sub>2</sub> exhibited a proton conductivity of up to  $8.24 \times 10^{-2} \text{ S cm}^{-1}$  (SD =  $\pm 0.031$ ) at 353 K under 98% relative humidity (RH), which was more than two orders of magnitude higher than that of its  $-\text{SO}_3\text{H}$ -free analogue, PP-(Ph)<sub>2</sub> ( $2.32 \times 10^{-4} \text{ S cm}^{-1}$ ) (SD =  $\pm 0.019$ ) under identical conditions. Therefore, for application in a PEM fuel cell, PP-(PhSO<sub>3</sub>H)<sub>2</sub>-based matrix-mixed membranes (PP-(PhSO<sub>3</sub>H)<sub>2</sub>-MMMs) were fabricated by mixing them with polyacrylonitrile (PAN) in various ratios. The proton conductivity could reach up to  $6.11 \times 10^{-2} \text{ S cm}^{-1}$  (SD =  $\pm 0.0048$ ) at 353 K and 98%RH, when the weight ratio of PP-(PhSO<sub>3</sub>H)<sub>2</sub>:PAN was 3:1, the value of which was comparable with those of commercially available electrolytes used in PEM fuel cells. PP-(PhSO<sub>3</sub>H)<sub>2</sub>-MMM (3:1) had an extended lifetime of reusability. Using phosphazene and bisulfonated multiple-amine modules as precursors, we demonstrated that a porous organic polymer with a highly effective proton-conductive matrix-mixed membrane for PEM fuel cells could be produced readily by an intuitive polymeric reaction.

 Received 18th October 2023  
 Accepted 11th April 2024

DOI: 10.1039/d3ra07094h

[rsc.li/rsc-advances](http://rsc.li/rsc-advances)

## Introduction

The global increase in use of conventional fossil fuels has resulted in several major environmental challenges, including pollution of air, water, and soil, and has degraded human life inexorably. As a result, clean and renewable energy resources are highly demanded for a sustainable future.<sup>1,2</sup>

Hydrogen is widely recognized as one of the most sustainable and clean energy carriers capable of permanently alleviating the environmental challenges caused by conventional fossil fuels and achieving carbon neutrality.<sup>3-6</sup> Using H<sub>2</sub> as fuel, proton-exchange membrane (PEM) fuel cells can be used to convert the chemical energy directly into electricity with high

efficiency and no carbon emissions. Therefore, PEMs have a major contribution to the overall efficiency of PEM fuel cells. Because of their comparatively high proton conductivity at low temperatures, PEMs are the most promising membranes for automotive applications and are utilized in PEM fuel cells. A range of polymeric materials have been utilized in the production of different types of polymeric membranes, including the Nafion® membrane (115, 117, 211, and 212). This commercially available product, manufactured by Dupont, is commonly employed in various applications due to its remarkable chemical and thermal stability, strong mechanical properties, and excellent proton conductivity.<sup>7,8</sup> However, the widespread use of PEMs is limited due to their high cost and the challenges associated with their synthesis. There are some limitations linked to this methodology, notably the cost ramifications and the challenge of effectively managing waste. The presence of fluorine within the structural framework may result in substantial expenditures associated with the disposal of outdated materials.<sup>9</sup> Hence, there is a need for the fabrication of polyphosphazene-based membranes by cost-effective and straightforward synthesis of alternative polymeric materials

*Department of Mechanical and Energy Engineering, Key Laboratory of Energy Conversion and Storage Technologies, Southern University of Science and Technology, Shenzhen, 518055, China. E-mail: wanghj@sustech.edu.cn*

† Electronic supplementary information (ESI) available: Experimental section, table summary of temperature-dependent proton conductivities, figures of FTIR, PXRD, N<sub>2</sub> sorption isotherms, PP-(Ph)<sub>2</sub>-MMM and PP-(PhSO<sub>3</sub>H)<sub>2</sub>-MMM photographs (PDF). See DOI: <https://doi.org/10.1039/d3ra07094h>



derived from bisulfonated polyphosphazene to facilitate the commercial utilization of PEMs. The development of innovative proton-conductive electrolytes, namely those based on bisulfonated polyphosphazene, is crucial for ensuring the practicality and effectiveness of PEM fuel cells.<sup>10–14</sup>

Typically, porous materials permit the loading of bulky visitors and endow composites with multiple functionalities. Numerous porous materials based on coordination, covalent, and hydrogen bonds have been synthesized and put to extensive use.<sup>15–18</sup> Nafion, a perfluorinated sulfonated polymeric electrolyte, has been utilized as a PEM material recently due to its high proton conductivity and durability. However, its prospective large-scale practical application is hampered by its high cost, synthetic hitches, and restricted working conditions.<sup>19–21</sup> In response to the success of Nafion, numerous inorganic metal compounds, graphdiynes,<sup>22,23</sup> polyoxometalates,<sup>24,25</sup> and materials with  $-\text{SO}_3\text{H}$  functionalities<sup>26–28</sup> have been incorporated into porous materials as Nafion substitutes to address their fabrication and application issues.<sup>29–35</sup> Using the Cu(I)-CAAC click reaction,<sup>36–40</sup> we grafted  $-\text{SO}_3\text{H}$  groups into the skeletons of two robust porous materials, a triazole-based porous organic polymer (TaPOP-1) and a metal-organic framework (UiO-66), during an *in situ* synthesis or by post-treatment, respectively. In both sulfonated porous samples, TaPOP-1- $\text{SO}_3\text{H}$  and UiO-66- $\text{SO}_3\text{H}$ , remarkable enhancements in proton conductivity were attained.<sup>36,37</sup> Even though numerous porous materials have been developed and studied for the application of proton-conduction, effective proton-conductive electrolytes derived from inexpensive reactants and prepared by simple methods are essential to meet the large-scale production of PEM fuel cells.

Polyphosphazenes are a class of robust polymers that can be produced at large scale for various applications. Usually, phosphazene units are connected by rigid linkers to form porous materials by incorporating  $-\text{SO}_3\text{H}$  functionalities simultaneously into their skeletons to form porous polyphosphazene for efficient proton conduction. Herein, we demonstrated fabrication of a porous organic polyphosphazene with  $-\text{SO}_3\text{H}$  constituents, designated PP-( $\text{PhSO}_3\text{H}$ )<sub>2</sub>, as an efficient PEM. PP-( $\text{PhSO}_3\text{H}$ )<sub>2</sub> was synthesized by combining hexachlorocyclo-triphosphazene (HCCP) and 4,4-diamino-2,2-biphenyldisulfonic acid in a simple, one-pot polymeric reaction. Physical characterizations showed that it is an organic polymer with a porous structure and a high degree of stability. It exhibited a proton conductivity of  $8.24 \times 10^{-2} \text{ S cm}^{-1}$  at 353 K under 98% relative humidity (RH), which is more than two orders of magnitude greater than its  $-\text{SO}_3\text{H}$ -free analogue, PP-(Ph)<sub>2</sub> ( $2.32 \times 10^{-4} \text{ S cm}^{-1}$ ), at the same temperature and humidity. When incorporated into matrix-mixed membranes with varying proportions of polyacrylonitrile (PAN), values comparable with those of commercially available proton-conductive electrolytes were observed under practical operating conditions. This result demonstrated that by incorporating  $-\text{SO}_3\text{H}$  moieties into the scaffolds of phosphazene-based porous organic polymers, proton-conductive electrolytes suitable for use in PEM fuel cells could be manufactured.

## Materials and reagents

All the chemicals, reagents, and solvents used for the syntheses of materials were available commercially and were used as received unless stated otherwise. 4,4-Diamino-2,2-biphenyldisulfonic acid (85%), potassium carbonate (99.5%), benzidine (98%), and polyacrylonitrile (98%) were purchased from Aladdin Bio-Chem Technology (Shanghai, China). Anhydrous DMSO, anhydrous DMF, and  $\text{H}_2\text{SO}_4$  were purchased from Shanghai Macklin Biochemicals (Beijing, China).

## Experimental methods

**Synthesis of PP-( $\text{PhSO}_3\text{H}$ )<sub>2</sub>.** In a two-necked round-bottomed flask (100 mL), 3.1 g of 4,4-diamino-2,2-biphenyldisulfonic acid (9 mmol), 0.62 g of potassium carbonate (4.5 mmol), and 45 mL of anhydrous DMSO were added. Then, 1.043 g of hexachlorocyclo-triphosphazene (HCCP) (3 mmol) in 20 mL of anhydrous DMSO was added dropwise to the flask under stirring. After stirring and reflux at 125 °C for 6 h in a  $\text{N}_2$  atmosphere, a solid powder was generated (Fig. 1). Collection by centrifugation and washing by an aqueous solution of 0.1 M  $\text{H}_2\text{SO}_4$ , ethanol, and then acetone (three times for each solvent) and drying overnight in a vacuum oven at 75 °C was done. A fine blackish powder of PP-( $\text{PhSO}_3\text{H}$ )<sub>2</sub> was obtained in a yield of 76% based on the starting reactants.

**Synthesis of PP-(Ph)<sub>2</sub>.** The synthetic procedure was similar to that of PP-( $\text{PhSO}_3\text{H}$ )<sub>2</sub>. Benzidine (9 mmol, 1.67 g), potassium carbonate (4.5 mmol), and 45 mL of anhydrous DMSO were added to a two-neck round-bottomed flask, followed by dropwise addition of an anhydrous DMSO solution of HCCP (3 mmol, 1.043 g) under stirring in a  $\text{N}_2$  atmosphere. After 6 h of reflux at 125 °C, the particulate was collected by centrifugation and washed with an aqueous solution of 0.1 M  $\text{H}_2\text{SO}_4$ , ethanol, and then acetone (three times for each solvent). After drying overnight at 75 °C in a vacuum oven, fine PP-(Ph)<sub>2</sub> powder was ultimately obtained.

**Fabrication of matrix-mixed membranes.** Polyacrylonitrile was used to form casting solutions as a polymer matrix. PAN (300 mg) was first dissolved in DMF (2 mL) and placed in an oven overnight at 70 °C to obtain a clear slurry. Then, the fabricated PP-( $\text{PhSO}_3\text{H}$ )<sub>2</sub> or PP-(Ph)<sub>2</sub> was mixed with the clear PAN slurry in different ratios to obtain a homogeneous solution. The latter was placed across the surface of aluminium foil with a casting knife at a 100  $\mu\text{m}$  gap to enable formation of a film. After natural drying for 1 day, followed by immersion in water for an additional day to eliminate additives and solvents, matrix-mixed membranes were produced. These membranes could be preserved at room temperature provided they are well wrapped with aluminium foil (Fig. S4†).

## Results and discussion

Hexachlorocyclo-triphosphazene and a rigid organic diamine with a  $-\text{SO}_3\text{H}$  functional group, 4,4-diamino-2,2-biphenyldisulfonic acid,<sup>26,29–32</sup> were chosen as precursors for the fabrication of a polyphosphazene-based porous organic



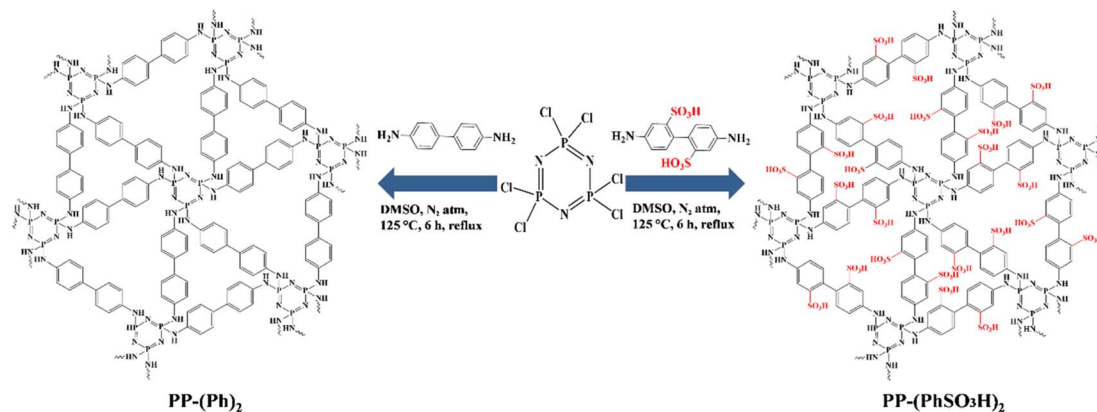


Fig. 1 Synthetic scheme of PP-(PhSO<sub>3</sub>H)<sub>2</sub>.

polymer. Fig. 1 depicts the PP-(PhSO<sub>3</sub>H)<sub>2</sub> fine black powder obtained after a simple one-pot polymeric reaction.<sup>40–42</sup> As a control, a sample of its –SO<sub>3</sub>H-free analogue, PP-(Ph)<sub>2</sub>, was also synthesized using the same method.

X-ray diffraction measurements revealed the amorphous morphology of powder samples (Fig. S1†). Scanning electron microscopy (SEM) images and energy dispersive X-ray (EDX) spectroscopy mapping analyses of PP-(PhSO<sub>3</sub>H)<sub>2</sub>, showed C, O, N, P, and S to be disseminated uniformly in the amorphous polymer (Fig. 3 and S2†). FTIR spectroscopy of PP-(PhSO<sub>3</sub>H)<sub>2</sub> and PP-(Ph)<sub>2</sub> demonstrated that the samples exhibited N=P bond vibrations at 1200 cm<sup>-1</sup> and 1264 cm<sup>-1</sup>, indicating the presence of polyphosphazene moieties in PP-(PhSO<sub>3</sub>H)<sub>2</sub> and PP-(Ph)<sub>2</sub> (Fig. 2 and S3†).<sup>40–42</sup> The peaks at 3448 cm<sup>-1</sup> and 3352 cm<sup>-1</sup> in PP-(PhSO<sub>3</sub>H)<sub>2</sub> and PP-(Ph)<sub>2</sub> were the stretching bands of N–H groups, indicating that the amino groups (–NH) had been incorporated into both samples. A peak at 1036 cm<sup>-1</sup> (–SO<sub>3</sub>H) unambiguously indicated a sulfonic acid group in PP-(PhSO<sub>3</sub>H)<sub>2</sub>, whereas PP-(Ph)<sub>2</sub> (ref. 33–35) lacked a corresponding peak. The incorporation of –SO<sub>3</sub>H functional groups into the synthesized PP-(PhSO<sub>3</sub>H)<sub>2</sub> was confirmed by FTIR spectroscopy.

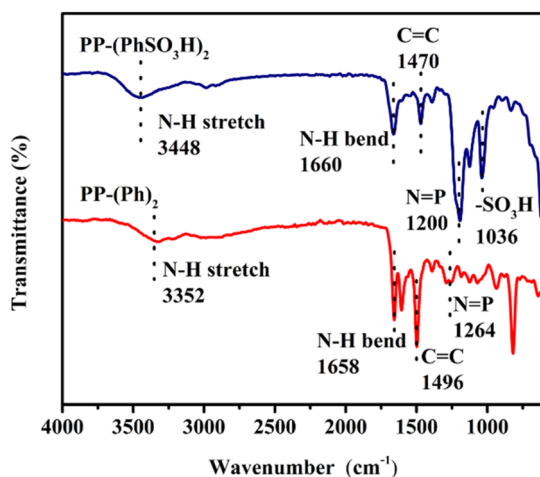


Fig. 2 FTIR spectra of PP-(PhSO<sub>3</sub>H)<sub>2</sub> and PP-(Ph)<sub>2</sub>.

N<sub>2</sub> sorption measurement showed a surface area of 28 m<sup>2</sup> g<sup>-1</sup> for PP-(PhSO<sub>3</sub>H)<sub>2</sub> and 35 m<sup>2</sup> g<sup>-1</sup> for PP-(Ph)<sub>2</sub> (Fig. 4a).<sup>43</sup> Thermogravimetric analyses were carried out to examine their thermal stability. Weight losses were observed in both samples along with a temperature increase (0–120 °C) attributed to evaporation of absorbed water and solvent molecules (Fig. 4b). Significant weight losses up to ~400 °C were due to polymer degradation, which revealed the thermal stability of polyphosphazenes below 120 °C, which is working temperature of a PEM fuel cell.<sup>10–12</sup>

The proton conductivities of the two samples were evaluated using electrochemical impedance spectroscopy (EIS) under different temperatures (303 K to 353 K) and RH (75%RH to 98% RH) after they had been pressed into tablets. The obtained curves revealed that the proton conductivity of PP-(PhSO<sub>3</sub>H)<sub>2</sub> exhibited a positive connection with temperature and RH (Fig. 5 and Table 1). At 80 °C and 98% RH, the proton conductivity of PP-(PhSO<sub>3</sub>H)<sub>2</sub> increased to 8.24 × 10<sup>-2</sup> S cm<sup>-1</sup>, which was more than two orders of magnitude greater than the proton conductivity of PP-(Ph)<sub>2</sub> under the same circumstances (2.32 × 10<sup>-4</sup> S cm<sup>-1</sup>).<sup>23–25</sup> Following that, Arrhenius plots based on proton conductivity were built, and activation-energy values were obtained using the least-squares fitting approach. Values were 0.28, 0.22, and 0.16 eV for the synthesized PP-(PhSO<sub>3</sub>H)<sub>2</sub> when measured at 98%RH, 85%RH, and 75%RH, respectively (Fig. 5d). We concluded that proton transport within the synthesized PP-(PhSO<sub>3</sub>H)<sub>2</sub> followed the Grotthuss mechanism.<sup>44–48</sup> The insertion of *in situ*-produced amine groups caused the synthesized PP-(PhSO<sub>3</sub>H)<sub>2</sub> to have an affinity link to the water molecule adsorbed in its pores. Concurrently, the built-in –SO<sub>3</sub>H moieties could offer exceptionally active free-moving protons, which improved the efficiency of proton conduction. As a result of the synergistic impact of the *in situ*-generated amine groups and in-built –SO<sub>3</sub>H moieties, the manufactured PP-(PhSO<sub>3</sub>H)<sub>2</sub> had high proton conductivity, making it a very promising prospective electrolyte for use in PEM fuel cells.

PAN was chosen as the casting solution in membrane fabrications with the PP-(PhSO<sub>3</sub>H)<sub>2</sub> as the core electrolyte mixed in various weight ratios to form matrix-mixed membranes PP-



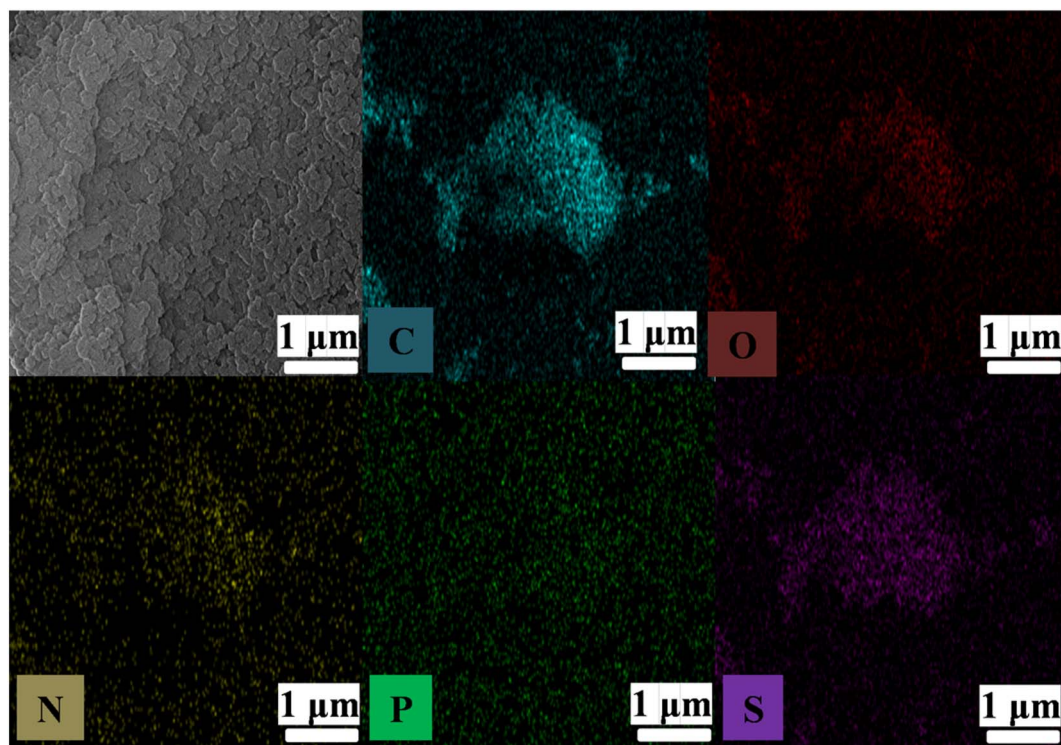


Fig. 3 Energy-dispersive X-ray mapping of PP-(PhSO<sub>3</sub>H)<sub>2</sub>.

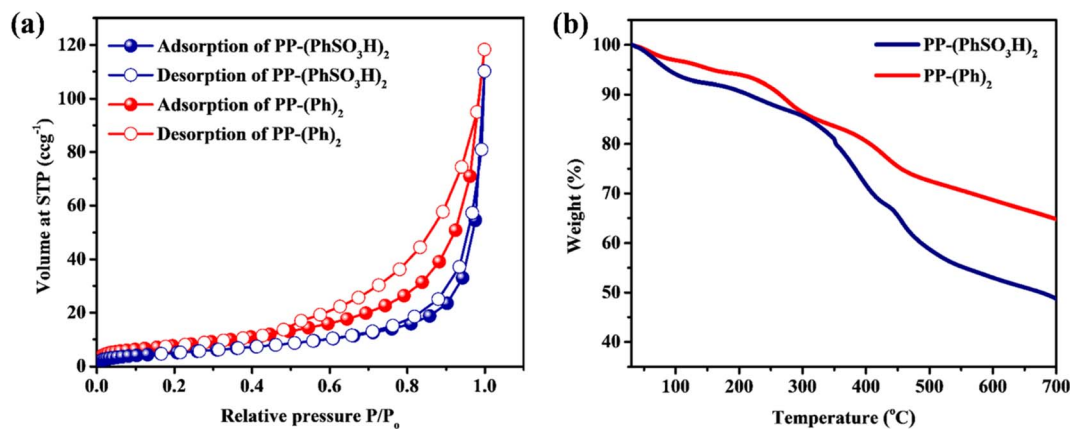


Fig. 4 (a) N<sub>2</sub> sorption isotherms and (b) TGA curves of PP-(PhSO<sub>3</sub>H)<sub>2</sub> and PP-(Ph)<sub>2</sub>.

(PhSO<sub>3</sub>H)<sub>2</sub>-PAN (*n* : *m*) (where *n* : *m* represents the weight ratios of PP-(PhSO<sub>3</sub>H)<sub>2</sub> : PAN) after painting, drying, and soaking.<sup>26–28,49–52</sup> When the ratio of PP-(PhSO<sub>3</sub>H)<sub>2</sub> to PAN in matrix-mixed membranes exceeded 4 : 1, membrane fragility began to set in. Therefore, membranes with PP-(PhSO<sub>3</sub>H)<sub>2</sub> and PAN weight ratios of 1 : 1 and 3 : 1 were manufactured (Fig. 6a). The morphology of the fabricated PP-(PhSO<sub>3</sub>H)<sub>2</sub>-PAN (3 : 1) was determined by SEM. It showed a smooth and uniform surface with the thickness of ~60.20 μm (Fig. 6b).

The physical properties of the membranes were evaluated using documented standard procedures.<sup>26–28,53–56</sup> To identify the active -SO<sub>3</sub>H groups in manufactured membranes, their ion

exchange capacity (IEC) was first determined by acid-base titration.<sup>26–28,53,54</sup> Using an aqueous solution of 0.01 M NaOH as the titrant solution and phenolphthalein as the indicator, titration experiments were conducted after ion exchange to exchange the proton in the membranes with sodium ions in the prepared NaCl solutions (see the experimental section of ESI† for additional information). According to Table 2, the calculated results of titration experiments revealed that the IEC of manufactured matrix-mixed membranes increased from 0.58 mmol g<sup>-1</sup> of PP-(PhSO<sub>3</sub>H)<sub>2</sub>-PAN (0.1 : 1) to 2.81 mmol g<sup>-1</sup> of PP-(PhSO<sub>3</sub>H)<sub>2</sub>-PAN (3 : 1).



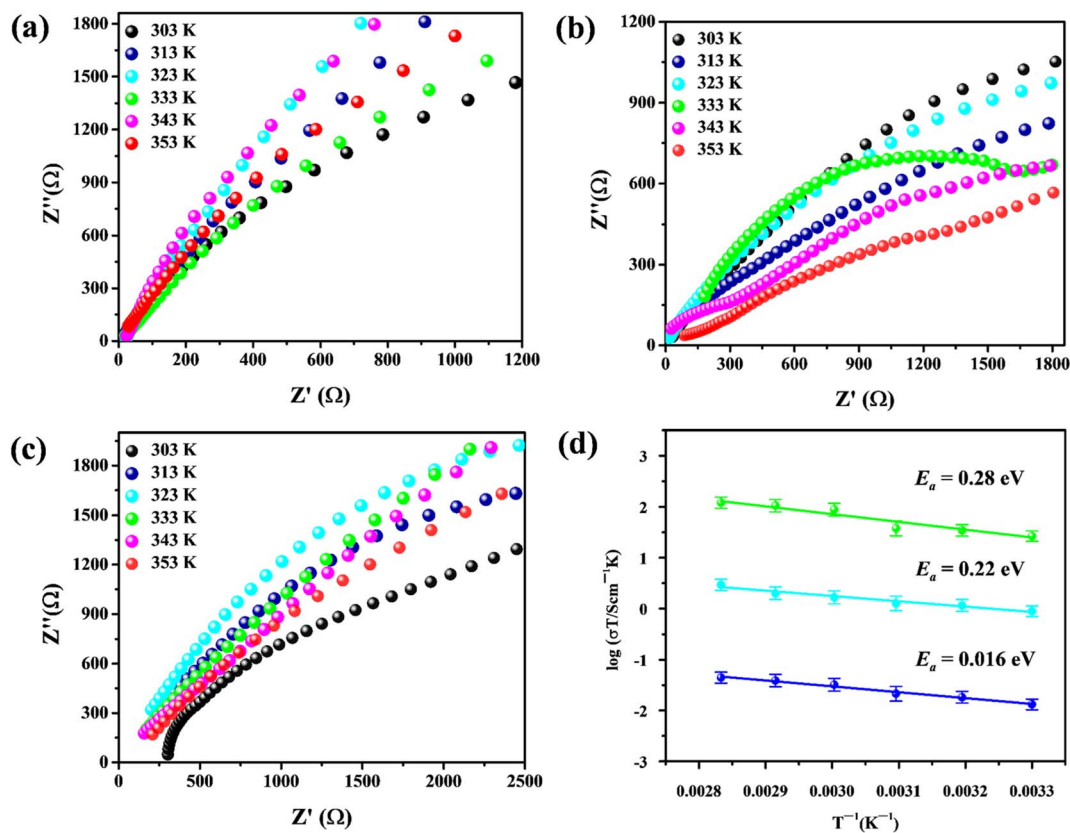


Fig. 5 Nyquist plots of PP-(PhSO<sub>3</sub>H)<sub>2</sub> measured at different temperatures and different relative humidities. (a) 98%RH, (b) 85%RH, (c) 75%RH. (d) Arrhenius plots of proton conductivity for PP-(PhSO<sub>3</sub>H)<sub>2</sub> at 98% RH (green), 85% RH (cyan), and 75% RH (blue).

Table 1 Proton conductivities (S cm<sup>-1</sup>) of synthesized PP-(PhSO<sub>3</sub>H)<sub>2</sub> under different conditions of temperature and relative humidity

<i>T</i>	98%RH SD <sup>a</sup> = ±0.031	85%RH SD = ±0.0026	75%RH SD = ±0.005
80 °C	8.24 × 10 <sup>-2</sup>	8.11 × 10 <sup>-3</sup>	3.65 × 10 <sup>-3</sup>
70 °C	5.16 × 10 <sup>-2</sup>	6.58 × 10 <sup>-3</sup>	2.83 × 10 <sup>-3</sup>
60 °C	3.25 × 10 <sup>-2</sup>	5.79 × 10 <sup>-3</sup>	1.38 × 10 <sup>-4</sup>
50 °C	1.89 × 10 <sup>-2</sup>	4.55 × 10 <sup>-3</sup>	9.85 × 10 <sup>-4</sup>
40 °C	8.81 × 10 <sup>-3</sup>	3.91 × 10 <sup>-3</sup>	8.66 × 10 <sup>-4</sup>
30 °C	6.29 × 10 <sup>-3</sup>	1.84 × 10 <sup>-3</sup>	6.57 × 10 <sup>-4</sup>

<sup>a</sup> SD denotes the standard deviation of the values of proton conductivity.

Water uptake (WU) is a critical factor for matrix-mixed membranes because it determines proton conduction. WU is analyzed by weight differences between dry and hydrated samples after overnight immersion in deionized H<sub>2</sub>O at 30 or 80 °C.<sup>26–28,53–56</sup> As shown in Table 2, at the same temperature, all of the manufactured membranes had enhanced water absorption as the temperature increased, with the WU value of PP-(PhSO<sub>3</sub>H)<sub>2</sub>-PAN (3:1) increasing up to 23% at 80 °C. The dimensional stability and swelling ratios of all membranes were measured by comparing dried and hydrated samples (see the experimental section of ESI† for additional information).<sup>26–28,53–56</sup> The dimensional differences demonstrated that all the fabricated membranes were less than 2.8% and 3.2% at 30 and 80 °C, respectively, indicating high

dimensional stability. All membranes swelled less than 1.70% and 2.65% at 30 and 80 °C, respectively, indicating their strong dimensional stability.

The chemical and hydrolytic stability of all matrix-mixed membranes was investigated by treatment with different reagents (see the experimental section of ESI† for additional information). Their oxidative chemical stability was tested after immersion in Fenton reagent (FeSO<sub>4</sub> in 3% H<sub>2</sub>O<sub>2</sub>, 3.0 ppm) based on the time (*t*) it took for the membranes to totally disintegrate at various temperatures.<sup>26–28,55</sup> As indicated in Table 3, the elapsed periods (*t*) increased from 8 h of PP-(PhSO<sub>3</sub>H)<sub>2</sub>-PAN (0.1:1) at 80 °C to 36 h of PP-(PhSO<sub>3</sub>H)<sub>2</sub>-PAN (3:1) at 30 °C. The prolonged time it took for the membranes to lose their mechanical capability was also evaluated by submersion in



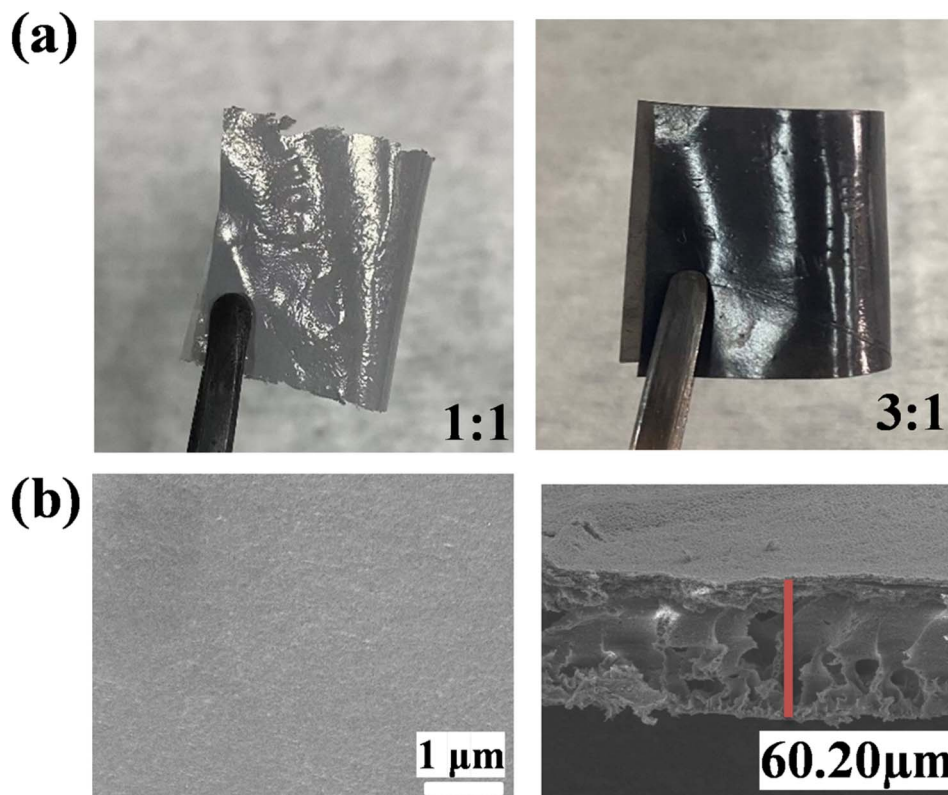


Fig. 6 (a) Photographs and (b) SEM images of PP-(PhSO<sub>3</sub>H)<sub>2</sub>-PAN (3 : 1) showing its upper surface (left) and its thickness (right).

Table 2 Ion exchange capacity, water uptake, dimensional stability, and swelling ratios of fabricated membranes

Membranes	IEC (mmol g <sup>-1</sup> )		WU (%)		Dimensional stability (%)				Swelling ratio (%)	
	IEC <sub>T</sub>	IEC <sub>Exp.</sub>	30 °C	80 °C	(ΔL <sub>c</sub> )		(ΔW <sub>c</sub> )		30 °C	80 °C
					30 °C	80 °C	30 °C	80 °C		
PP-(PhSO <sub>3</sub> H) <sub>2</sub> -PAN (3 : 1)	2.86	2.81	13.13	22.61	1.92	2.83	2.50	3.15	1.65	2.62
PP-(PhSO <sub>3</sub> H) <sub>2</sub> -PAN (1 : 1)	1.98	1.91	8.73	14.68	1.55	1.93	1.63	2.09	0.95	1.42
PP-(PhSO <sub>3</sub> H) <sub>2</sub> -PAN (0.4 : 1)	0.87	0.83	6.59	9.91	0.81	1.07	1.44	1.97	0.51	0.97
PP-(PhSO <sub>3</sub> H) <sub>2</sub> -PAN (0.1 : 1)	0.63	0.58	3.66	7.22	0.66	0.89	0.71	0.90	0.32	0.63

distilled water at 50 °C (Table 3).<sup>26–28,56</sup> These values were >96 h, and the membrane of PP-(PhSO<sub>3</sub>H)<sub>2</sub>-PAN (3 : 1) had an elapsed duration of up to 120 h, which revealed excellent physico-chemical features towards PEM fuel cells.

Finally, the proton conductivity of constructed membranes was measured *via* EIS where the conductivity of

Table 3 Chemical and hydrolytic stability of fabricated membranes

Membranes	Chemical stability/ <i>t</i> (h)		Hydrolytic stability/ <i>t</i> (h)
	30 °C	80 °C	50 °C
PP-(PhSO <sub>3</sub> H) <sub>2</sub> -PAN (3 : 1)	36	18	120
PP-(PhSO <sub>3</sub> H) <sub>2</sub> -PAN (1 : 1)	36	18	120
PP-(PhSO <sub>3</sub> H) <sub>2</sub> -PAN (0.4 : 1)	36	12	96
PP-(PhSO <sub>3</sub> H) <sub>2</sub> -PAN (0.1 : 1)	36	8	96

PP-(PhSO<sub>3</sub>H)<sub>2</sub>-PAN (3 : 1) was up to  $6.11 \times 10^{-2} \text{ S cm}^{-1}$  at 80 °C and 98% RH (Fig. 7a and Table 4). This value is close to that of the PEM membranes Nafion-type electrolyte and marketed Nafion®117,<sup>57,58</sup> *i.e.*,  $5 \times 10^{-2}$  and  $1.5 \times 10^{-1} \text{ S cm}^{-1}$  at 30 and 80 °C, respectively, at 98% RH (Table S1†). Similarly, the graph of proton conductivity *versus* time for PP-(PhSO<sub>3</sub>H)<sub>2</sub>-PAN (3 : 1) suggested that it had long-term stability (Fig. 7b). Other matrix-mixed membranes (1 : 1, 0.4 : 1, 0.1 : 1) also showed adequate proton conductivity with long-life durability (Table 4). Bisulfonated polyphosphazenes have appealing potential as proton-conductive electrolytes for PEM fuel cells due to their excellent proton conduction, low cost, and facile production. Our study may provide a simple polymeric process employing bisulfonated modules as precursors for effective and economically feasible proton-conductive electrolytes for PEM fuel cells.



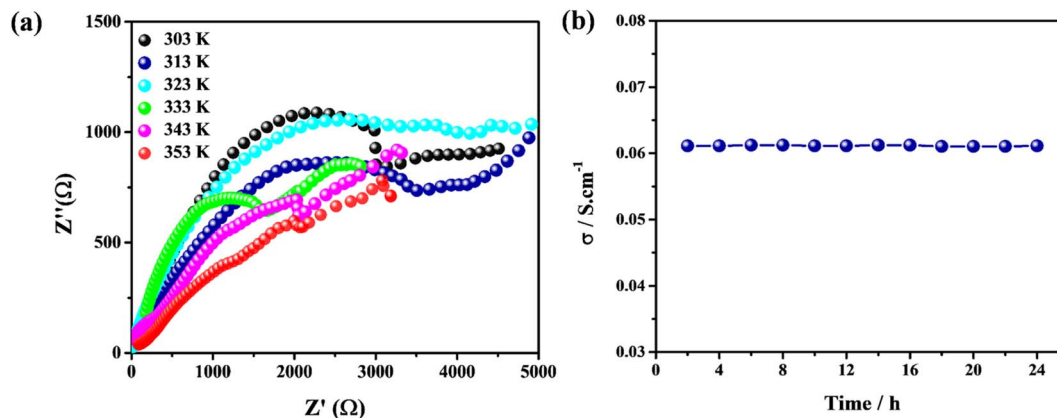


Fig. 7 (a) Nyquist plot of PP-(PhSO<sub>3</sub>H)<sub>2</sub>-PAN (3 : 1) at various temperatures and 98%RH. (b) Long-life reusability of PP-(PhSO<sub>3</sub>H)<sub>2</sub>-PAN (3 : 1) at 80 °C and 98%RH.

Table 4 Proton conductivity (S cm<sup>-1</sup>) of synthesized membranes under 98%RH

Temperature	PP-(PhSO <sub>3</sub> H) <sub>2</sub> -PAN (0.1 : 1) SD <sup>a</sup> = ±0.0065	PP-(PhSO <sub>3</sub> H) <sub>2</sub> -PAN (0.4 : 1) SD = ±0.0045	PP-(PhSO <sub>3</sub> H) <sub>2</sub> -PAN (1 : 1) SD = ±0.0032	PP-(PhSO <sub>3</sub> H) <sub>2</sub> -PAN (3 : 1) SD = ±0.0048
80 °C	$8.52 \times 10^{-3}$	$2.32 \times 10^{-2}$	$4.22 \times 10^{-2}$	$6.11 \times 10^{-2}$
70 °C	$7.98 \times 10^{-3}$	$2.06 \times 10^{-2}$	$3.83 \times 10^{-2}$	$5.64 \times 10^{-2}$
60 °C	$7.22 \times 10^{-3}$	$1.82 \times 10^{-2}$	$3.07 \times 10^{-2}$	$4.92 \times 10^{-2}$
50 °C	$6.08 \times 10^{-3}$	$1.11 \times 10^{-2}$	$2.75 \times 10^{-2}$	$4.61 \times 10^{-2}$
40 °C	$5.85 \times 10^{-3}$	$9.88 \times 10^{-3}$	$2.02 \times 10^{-2}$	$4.05 \times 10^{-2}$
30 °C	$5.13 \times 10^{-3}$	$9.17 \times 10^{-3}$	$1.87 \times 10^{-2}$	$3.93 \times 10^{-2}$

<sup>a</sup> SD denotes the standard deviation of the proton conductivity.

## Conclusions

A bisulfonated polyphosphazene-based porous organic polymer with built-in -SO<sub>3</sub>H moieties was produced as a proton-conductive electrolyte for use in PEM fuel cells using a simple one-pot polymeric method. Experiments on proton conductivity indicated a value of  $8.24 \times 10^{-2}$  S cm<sup>-1</sup> at 353 K under 98% RH, which is more than two orders of magnitude greater than that of its -SO<sub>3</sub>H-free equivalent under identical conditions. Fabricated matrix-mixed membranes showed proton conductivity of up to  $6.11 \times 10^{-2}$  S cm<sup>-1</sup> at 353 K and 98% RH, which is equivalent to that of commercially available proton-conductive electrolytes. Bisulfonated polyphosphazenes with -SO<sub>3</sub>H have huge potential as proton-conductive electrolytes. This research provides insight on the manufacture of low-cost proton-conductive membranes for use in PEM fuel cells.

## Author contributions

The manuscript was written through the contributions of all authors. All authors have given approval to the final version of the manuscript.

## Conflicts of interest

There are no conflicts to declare.

## Acknowledgements

This work was supported by the Ministry of Education Key Laboratory of Energy Conversion and Storage Technologies (Y01406010), Guangdong Innovative and Entrepreneurial Research Team Program (2016ZT06N500), and Guangdong Provincial Key Laboratory of Energy Materials for Electric Power (2018B030322001).

## References

- W. Gao, S. Liang, R. Wang, Q. Jiang, Y. Zhang, Q. Zheng, B. Xie, C. Y. Toe, X. Zhu, J. Wang, *et al.*, Industrial carbon dioxide capture and utilization: state of the art and future challenges, *Chem. Soc. Rev.*, 2020, **49**, 8584–8686.
- H. Li, C. Qiu, S. Ren, Q. Dong, S. Zhang, F. Zhou, X. Liang, J. Wang, S. Li and M. Yu, Na<sup>+</sup>-gated water-conducting nanochannels for boosting CO<sub>2</sub> conversion to liquid fuels, *Science*, 2020, **367**, 667–671.
- F. Chang, W. Gao, J. Guo and P. Chen, Emerging materials and methods toward ammonia-based energy storage and conversion, *Adv. Mater.*, 2021, **33**, 2005721.
- C. Wang, Q. Wang, F. Fu and D. Astruc, Hydrogen generation upon nanocatalyzed hydrolysis of hydrogen-rich boron derivatives: recent developments, *Acc. Chem. Res.*, 2020, **53**, 2483–2493.



- 5 M. Z. Rahman, M. G. Kibria and C. B. Mullins, Metal-free photocatalysts for hydrogen evolution, *Chem. Soc. Rev.*, 2020, **49**, 1887–1931.
- 6 Y. Lei, Y. Wang, Y. Liu, C. Song, Q. Li, D. Wang and Y. Li, Designing atomic active centers for hydrogen evolution electrocatalysts, *Angew. Chem., Int. Ed.*, 2020, **59**, 20794–20812.
- 7 A. Ursua, L. M. Gandia and P. Sanchis, Hydrogen production from water electrolysis: current status and future trends, *Proc. IEEE*, 2012, **100**, 410–426.
- 8 A. Goñi-Urtiaga, D. Presvytes and K. Scott, Solid acids as electrolyte materials for proton exchange membrane (PEM) electrolysis: review, *Int. J. Hydrogen Energy*, 2012, **37**, 3358–3372.
- 9 G. Wei, L. Xu, C. Huang and Y. Wang, SPE water electrolysis with SPEEK/PES blend membrane, *Int. J. Hydrogen Energy*, 2010, **35**, 7778–7783.
- 10 K.-D. Kreuer, S. J. Paddison, E. Spohr and M. Schuster, Transport in proton conductors for fuel-cell applications: simulations, elementary reactions, and phenomenology, *Chem. Rev.*, 2004, **104**, 4637–4678.
- 11 A. Kraysberg and Y. Ein-Eli, Review of advanced materials for proton exchange membrane fuel cells, *Energy Fuels*, 2014, **28**, 7303–7330.
- 12 Y. Wang, D. F. Ruiz Diaz, K. S. Chen, Z. Wang and X. C. Adroher, Materials, technological status, and fundamentals of PEM fuel cells – a review, *Mater. Today*, 2020, **32**, 178–203.
- 13 M. Ray, P. K. Samantaray and Y. S. Negi, In situ polymerization-mediated cross-linking of the MOF using poly(1-vinylimidazole) in SPEEK fuel cells, *ACS Appl. Polym. Mater.*, 2023, **5**, 4704–4715.
- 14 J. Li, W. Wang, Z. Jiang, B. Deng and Z.-j. Jiang, Co-filling of ZIFs-derived porous carbon and silica in improvement of sulfonated poly(ether ether ketone) as proton exchange membranes for direct methanol fuel cells, *J. Power Sources*, 2022, **543**, 231853.
- 15 J.-S. M. Lee, K.-i. Otake and S. Kitagawa, Transport properties in porous coordination polymers, *Coord. Chem. Rev.*, 2020, **421**, 213447.
- 16 D.-W. Lim and H. Kitagawa, Proton transport in metal-organic frameworks, *Chem. Rev.*, 2020, **120**, 8416–8467.
- 17 Y. Ye, L. Gong, S. Xiang, Z. Zhang and B. Chen, Metal-organic frameworks as a versatile platform for proton conductors, *Adv. Mater.*, 2020, **32**, 1907090.
- 18 A. Karmakar, R. Illathvalappil, B. Anothumakkool, A. Sen, P. Samanta, A. V. Desai, S. Kurungot and S. K. Ghosh, Hydrogen-bonded organic frameworks (HOFs): a new class of porous crystalline proton-conducting materials, *Angew. Chem., Int. Ed.*, 2016, **55**, 10667–10671.
- 19 K. A. Mauritz and R. B. Moore, State of understanding of Nafion, *Chem. Rev.*, 2004, **104**, 4535–4586.
- 20 X. Wu, X. Wang, G. He and J. Benziger, Differences in water sorption and proton conductivity between Nafion and SPEEK, *J. Polym. Sci., Part B: Polym. Phys.*, 2011, **49**, 1437–1445.
- 21 D. K. Paul, R. McCreery and K. Karan, Proton transport property in supported Nafion nanothin films by electrochemical impedance spectroscopy, *J. Electrochem. Soc.*, 2014, **161**, F1395.
- 22 L. Shi, A. Xu, D. Pan and T. Zhao, Aqueous proton-selective conduction across two-dimensional graphyne, *Nat. Commun.*, 2019, **10**, 1165.
- 23 J. Xu, H. Jiang, Y. Shen, X.-Z. Li, E. G. Wang and S. Meng, Transparent proton transport through a two-dimensional nanomesh material, *Nat. Commun.*, 2019, **10**, 3971.
- 24 M. Zhu, T. Iwano, M. Tan, D. Akutsu, S. Uchida, G. Chen and X. Fang, Macrocyclic polyoxometalates: selective polyanion binding and ultrahigh proton conduction, *Angew. Chem., Int. Ed.*, 2022, **61**, e202200666.
- 25 S. Li, Y. Zhao, S. Knoll, R. Liu, G. Li, Q. Peng, P. Qiu, D. He, C. Streb and X. Chen, High proton-conductivity in covalently linked polyoxometalate-organoboronic acid-polymers, *Angew. Chem., Int. Ed.*, 2021, **60**, 16953–16957.
- 26 J. Afzal, Y. Fu, T.-X. Luan, Z. Su and P.-Z. Li, Highly effective proton-conductive matrix-mixed membrane based on a –SO<sub>3</sub>H-functionalized polyphosphazene, *Langmuir*, 2022, **38**, 10503–10511.
- 27 J. Afzal, Y. Fu, T.-X. Luan, Z. Su and P.-Z. Li, Highly effective proton-conduction matrix-mixed membrane derived from an –SO<sub>3</sub>H functionalized polyamide, *Molecules*, 2022, **27**, 4110.
- 28 J. Afzal, Y. Fu, T.-X. Luan, D. Zhang, Y. Li, H. Li, K. Cheng, Z. Su and P.-Z. Li, Facile construction of a highly proton-conductive matrix-mixed membrane based on a –SO<sub>3</sub>H functionalized polyamide, *Soft Matter*, 2022, **18**, 5518–5523.
- 29 L. Liu, L. Yin, D. Cheng, S. Zhao, H.-Y. Zang, N. Zhang and G. Zhu, Surface-mediated construction of an ultrathin free-standing covalent organic framework membrane for efficient proton conduction, *Angew. Chem., Int. Ed.*, 2021, **60**, 14875–14880.
- 30 L. Cao, H. Wu, Y. Cao, C. Fan, R. Zhao, X. He, P. Yang, B. Shi, X. You and Z. Jiang, Weakly humidity-dependent proton-conducting COF membranes, *Adv. Mater.*, 2020, **32**, 2005565.
- 31 Y. Peng, G. Xu, Z. Hu, Y. Cheng, C. Chi, D. Yuan, H. Cheng and D. Zhao, Mechanoassisted synthesis of sulfonated covalent organic frameworks with high intrinsic proton conductivity, *ACS Appl. Mater. Interfaces*, 2016, **8**, 18505–18512.
- 32 S. Chandra, T. Kundu, K. Dey, M. Addicoat, T. Heine and R. Banerjee, Interplaying intrinsic and extrinsic proton conductivities in covalent organic frameworks, *Chem. Mater.*, 2016, **28**, 1489–1494.
- 33 S.-J. Yang, X. Ding and B.-H. Han, Conjugated microporous polymers with dense sulfonic acid groups as efficient proton conductors, *Langmuir*, 2018, **34**, 7640–7646.
- 34 M. Furtmair, J. Timm and R. Marschall, Sulfonation of porous materials and their proton conductivity, *Microporous Mesoporous Mater.*, 2021, **312**, 110745.
- 35 D. Zhang, Y. Gao, T.-X. Luan, K. Cheng, C. Li and P.-Z. Li, Facile construction of a click-based robust porous organic polymer and its in-situ sulfonation for proton conduction, *Microporous Mesoporous Mater.*, 2021, **325**, 111348.





- 36 X.-N. Zou, D. Zhang, Y. Xie, T.-X. Luan, W. Li, L. Li and P.-Z. Li, High enhancement in proton conductivity by incorporating sulfonic acids into a zirconium-based metal-organic framework via “click” reaction, *Inorg. Chem.*, 2021, **60**, 10089–10094.
- 37 P.-Z. Li, X.-J. Wang and Y. Zhao, Click chemistry as a versatile reaction for construction and modification of metal-organic frameworks, *Coord. Chem. Rev.*, 2019, **380**, 484–518.
- 38 P.-Z. Li, X.-J. Wang, J. Liu, J. S. Lim, R. Zou and Y. Zhao, A triazole-containing metal-organic framework as a highly effective and substrate size-dependent catalyst for CO<sub>2</sub> conversion, *J. Am. Chem. Soc.*, 2016, **138**, 2142–2145.
- 39 P.-Z. Li, X.-J. Wang, S. Y. Tan, C. Y. Ang, H. Chen, J. Liu, R. Zou and Y. Zhao, Clicked isoreticular metal-organic frameworks and their high performance in the selective capture and separation of large organic molecules, *Angew. Chem., Int. Ed.*, 2015, **54**, 12748–12752.
- 40 P. Dallas, J. Tucek, D. Jancik, M. Kolar, A. Panacek and R. Zboril, Magnetically controllable silver nanocomposite with multifunctional phosphotriazine matrix and high antimicrobial activity, *Adv. Funct. Mater.*, 2010, **20**, 2347–2354.
- 41 A. Zhang, Y. Bian, J. Wang, K. Chen, C. Dong and J. Ren, Suppressed blinking behavior of CdSe/CdS QDs by polymer coating, *Nanoscale*, 2016, **8**, 5006–5014.
- 42 H. Wang, H. Hu and Q. Peng, A facile one-step in-situ template strategy on the synthesis of cyclophosphazene-based amino-linked porous polymer and efficient removal of iodine, *Microporous Mesoporous Mater.*, 2021, **323**, 111249.
- 43 Y. Zhang, X. Chen, J. Xu, Q. Zhang, L. Gao, Z. Wang, L. Qu, K. Wang, Y. Li, Z. Cai, *et al.*, Cross-linked polyphosphazene nanospheres boosting long-lived organic room-temperature phosphorescence, *J. Am. Chem. Soc.*, 2022, **144**, 6107–6117.
- 44 K. S. W. Sing, Reporting physisorption data for gas/solid systems with special reference to the determination of surface area and porosity (Recommendations 1984), *Pure Appl. Chem.*, 1985, **57**, 603–619.
- 45 X. Meng, H.-N. Wang, S.-Y. Song and H.-J. Zhang, Proton-conducting crystalline porous materials, *Chem. Soc. Rev.*, 2017, **46**, 464–480.
- 46 G.-L. Hou and X.-B. Wang, Molecular specificity and proton transfer mechanisms in aerosol pre-nucleation clusters relevant to new particle formation, *Acc. Chem. Res.*, 2020, **53**, 2816–2827.
- 47 Y. Yang, P. Zhang, L. Hao, P. Cheng, Y. Chen and Z. Zhang, Grotthuss proton-conductive covalent organic frameworks for efficient proton pseudocapacitors, *Angew. Chem., Int. Ed.*, 2021, **60**, 21838–21845.
- 48 N. Agmon, The Grotthuss mechanism, *Chem. Phys. Lett.*, 1995, **244**, 456–462.
- 49 Y. Liu, M.-O. Coppens and Z. Jiang, Mixed-dimensional membranes: chemistry and structure–property relationships, *Chem. Soc. Rev.*, 2021, **50**, 11747–11765.
- 50 S. Zhang, S. Zhao, X. Jing, Z. Niu and X. Feng, Covalent organic framework-based membranes for liquid separation, *Org. Chem. Front.*, 2021, **8**, 3943–3967.
- 51 P. H. H. Duong, V. A. Kuehl, B. Mastorovich, J. O. Hoberg, B. A. Parkinson and K. D. Li-Oakey, Carboxyl-functionalized covalent organic framework as a two-dimensional nanofiller for mixed-matrix ultrafiltration membranes, *J. Membr. Sci.*, 2019, **574**, 338–348.
- 52 K. Duan, J. Wang, Y. Zhang and J. Liu, Covalent organic frameworks (COFs) functionalized mixed matrix membrane for effective CO<sub>2</sub>/N<sub>2</sub> separation, *J. Membr. Sci.*, 2019, **572**, 588–595.
- 53 M. I. Khan, M. Khraisheh and F. AlMomeni, Innovative BPPO anion exchange membranes formulation using diffusion dialysis-enhanced acid regeneration system, *Membranes*, 2021, **11**, 311.
- 54 F. Ali, S. Saeed, S. S. Shah, F. Rahim, L. Duclaux, J. M. Levêque and L. Reinert, Sulfonated polyimide-clay thin films for energy application, *Recent Pat. Nanotechnol.*, 2016, **10**, 221–230.
- 55 C. Wang, B. Shen, Y. Zhou, C. Xu, W. Chen, X. Zhao and J. Li, Sulfonated aromatic polyamides containing nitrile groups as proton exchange fuel cell membranes, *Int. J. Hydrogen Energy*, 2015, **40**, 6422–6429.
- 56 C. Wang, N. Li, D. W. Shin, S. Y. Lee, N. R. Kang, Y. M. Lee and M. D. Guiver, Fluorene-based poly(arylene ether sulfone)s containing clustered flexible pendant sulfonic acids as proton exchange membranes, *Macromolecules*, 2011, **44**, 7296–7306.
- 57 D. W. Kang, J. H. Song, K. J. Lee, H. G. Lee, J. E. Kim, H. Y. Lee, J. Y. Kim and C. S. Hong, A conductive porous organic polymer with superprotonic conductivity of a Nafion-type electrolyte, *J. Mater. Chem. A*, 2017, **5**, 17492–17498.
- 58 T. Suda, K. Yamazaki and H. Kawakami, Syntheses of sulfonated star-hyperbranched polyimides and their proton exchange membrane properties, *J. Power Sources*, 2010, **195**, 4641–4646.

